Journal of Thermal Analysis and Calorimetry, Vol. 70 (2002) 681–691

MISCIBILITY OF POLYMER BLENDS STUDIED BY A SIMPLIFIED METHOD OF DATA ANALYSIS USING LIGHT HEATING MODULATED TEMPERATURE DSC

Y. Saruyama[1*], *S. Wakiyama*[2] *and Y. Tsukahara*[2]

[1]Department of Polymer Science and Engineering, Kyoto Institute of Technology, Matsugasaki, Sakyo-ku, Kyoto 606-8585, Japan
[2]Department of Chemistry and Materials Technology, Kyoto Institute of Technology, Matsugasaki, Sakyo-ku, Kyoto 606-8585, Japan

Abstract

A simple method of application of light heating modulated temperature DSC to a study of miscibility of polymer blends has been developed. In this method only the sample was measured and the standard materials were not used. The total heat flow, the complex heat capacity, the reversing and non-reversing heat flows were obtained as values measured from those quantities in hypothetical glassy state at $T>T_g$. The values of the hypothetical glassy state were calculated by extrapolation from $T<T_g$. The present method gives relative values but useful information can be obtained from the results. Some results from miscible and immiscible polymer blends are shown.

Keywords: complex heat capacity, light heating modulated temperature DSC, miscibility of polymer blends, reversing and non-reversing heat flows

Introduction

We have applied light heating modulated temperature DSC (LMDSC) constructed in the author's (YS) laboratory [1, 2] to detailed studies of melting transition of polyethylene crystals [3]. In these studies measurement of standard materials as well as the samples [3, 5] or two types of measurement of the same sample (modulating both the sample and reference sides and only the sample side) [4] have been carried out. From these measurements new and useful information could be obtained. However, the measurement of the standard materials, that had to be made at every modulation frequency and in the temperature range applied to the sample, took long time. In the case of the method of reference 4 measurement of the same condition had to be made at least two times. The procedure of data processing was complicated and could not be finished in a short time. In the case of the conventional DSC useful information can often be obtained from measurement of only the sample without using the standard

* Author for correspondence: E-mail: Saruyama@ipc.kit.ac.jp

1418–2874/2002/ $ 5.00
Akadémiai Kiadó, Budapest

materials. In this work we investigated what types of information can be obtained from measurement of only the sample using LMDSC.

The samples used in this study were binary blends of a linear polystyrene and a multibranched polystyrene. The multibranched polystyrenes were poly(macromonomer)s synthesized from vinyl-terminated macromonomers. The chain polymerizations of vinyl-terminated macromonomers easily produce multibranched polymers of extremely high branch density [6–10], where every repeating unit of the backbone chain possesses one long branch at all times. The branch length and the branch number can be controlled by the molecular mass of the macromonomer and the polymerization conditions. Thus, poly(macromonomer)s are very interesting model polymers for investigation on the effect of branching architecture [11–14]. Previously, we revealed from the study on the glass transition temperature of the blends by conventional DSC measurement that the poly(macromonomer)s of polystyrene macromonomers showed immiscibility with the linear polystyrenes depending on the branching architecture of the poly(macromonomer)s and the molecular mass of the linear polystyrene [14]. This result is interesting because the monomeric units of both polymer components are styrene unit and thus the observed immiscibility between the polymer components results from the effect of the branching architecture. For further investigation on the miscible/immiscible behavior, LMDSC was applied to the multibranched/linear polymer blends in this study. Separation of the total heat flow to the reversing and non-reversing heat flows as well as measurement of the complex heat capacity was carried out to obtain more detailed information than the conventional DSC.

Experimental

Details of LMDSC instrument are explained in [1, 2]. Just a brief description is given here. LMDSC was constructed by combining a light source with a commercial heat flux DSC (Rigaku Thermo-Plus 8230). The light source was composed of a halogen lamp and two polarizers. One polarizer was fixed and the other was rotated by a motor. After passing through the polarizers the light intensity was modulated sinusoidally with time. The light was led to the sample chamber of the commercial DSC by optical fibers and irradiated the sample and the reference material through the glass windows made on the lid of the sample chamber. A disc shaped sample of ca 0.1 mm thick was put in an aluminum pan with an aluminum lid. Carbon was sprayed on the top surface of the lid for absorption of the light energy.

Binary (50/50% by mass) polymer blends of a linear polystyrene (LPSt70k) (Mw=7.9·10^4, Mw/Mn=1.18) with various poly(macromonomer)s were used as samples. The poly(macromonomer)s were synthesized as follows [8, 15]. ω-Methacryloyloxyethyl polystyrene macromonomers (MA-PSt)s were synthesized by the living anionic polymerization of styrene with *s*-BuLi followed by addition with ethylene oxide and termination with methacryloyl chloride. ω-vinylbenzyl polystyrene macromonomers (VB-PSt)s were synthesized by the living anionic polymerization of styrene with *s*-BuLi followed by termination with vinylbenzyl chloride. These macromonomers were polymerized using azobisisobutyronitrile (AIBN) initiator in benzene at 50–60°C for 24–48 h. Polymerization products were purified repeatedly by precipitation-extraction procedures

with cyclohexane-petroleum ether mixed solvents to remove unreacted macromonomers. Linear polystyrenes of different molecular masses were also synthesized by the living anionic polymerization technique. The mass average molecular mass, *Mw*, and the polydispersity index, *Mw*/*Mn*, of poly(macromonomer)s were determined by GPC (Tosoh HLC802A) equipped with a low angle laser light scattering (LALLS/Tosoh LS-8, He–Ne Laser) detector and a refractive index (RI) detector. The molecular structures of the poly(macromonomer)s are shown in Fig. 1. Values of *Mw*, *Mw*/*Mn*, *k*, the degree of polymerization of the poly(macromonomer)s and, *n*, the number of styrene units in the PSt branch, are summarized in Table 1. The *k* of the poly(macromonomer)s is equivalent to the number of PSt branch chains per molecule. The polymer blend samples were prepared by freeze drying the mixed benzene solution of the poly(macromonomer) and the linear polymer.

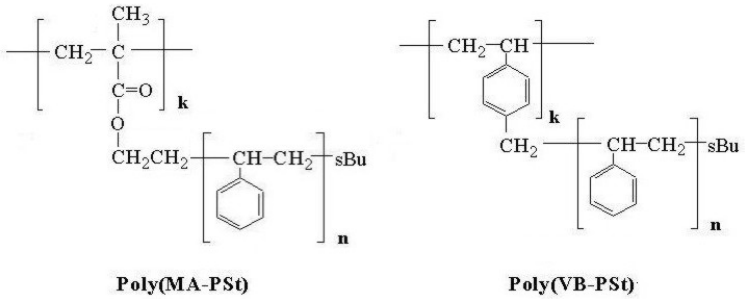

Fig. 1 Molecular structure of the poly(macromonomer)s

Table 1 Characterization of poly(macromonomer)s

Sample code	SEC-LALLS				
	$Mw \cdot 10^{-5}$	$Mn \cdot 10^{-5}$	*Mw*/*Mn*	*k*[a]	*n*[b]
Poly(MA-PSt1750)-2334	55.2	42.2	1.31	2334	16.8
Poly(MA-PSt2950)-600	20.4	13.5	1.51	600	28.4
Poly(MA-PSt4700)-930	71.3	48.3	1.48	930	45.2
Poly(VB-PSt1750)-197	4.18	3.67	1.14	167	16.8
Poly(VB-PSt2530)-570	15.5	12.4	1.25	507	24.3
Poly(VB-PSt6200)-739	40.0	30.6	1.31	739	59.6

[a]*k* is the number of side chains in one poly(macromonomer) molecule
[b]*n* is the number of styrene units per one side chain

Data analysis and results

All measurements were carried out irradiating only the sample side in the temperature range from 50 to 150°C including the glass transition temperatures of the polymer blends. In most cases the modulation period was 10 s. The modulation period of 3 and 30 s were used to study frequency dependence. Heating rate was 5 and 1 K min^{-1} to

obtain the total heat flow and the cyclic component, respectively. Different heating rate was used for good signal to noise ratio. After the heating process the sample was cooled to 50°C at 2 K min^{-1}.

The conventional DSC signal was extracted from the raw data by shift averaging over the modulation period. The cyclic component was obtained by reducing the conventional DSC signal from the raw data. The complex amplitude of the cyclic component was calculated by Fourier integral. These calculations were made during measurement in the personal computer connected to the LMDSC instrument. The con-

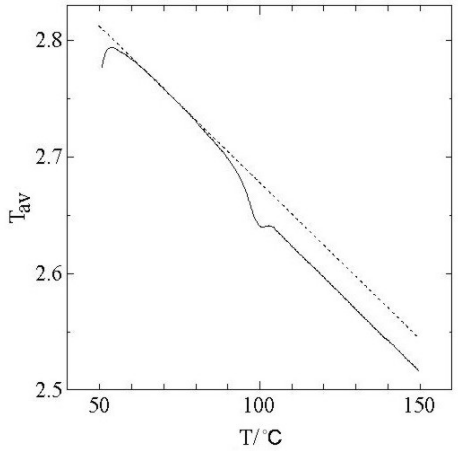

Fig. 2a Linear fitting (dotted) to the averaged signal, written as T_{av}, over the modulation period obtained from the blend of LPSt70k and Poly(VB-PSt2530)-570 in Table 1

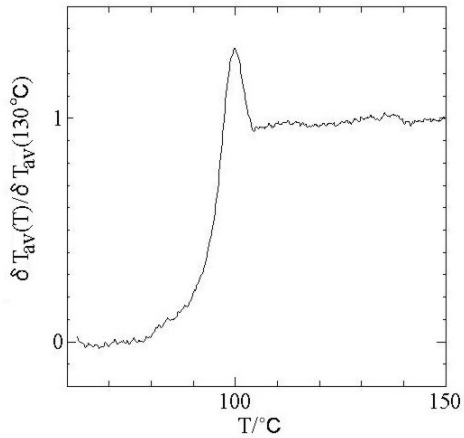

Fig. 2b Temperature dependence of the difference between the measured data and the fitted line, expressed as δT_{av}, scaled to the value at 130°C. Numeric values of the vertical axis of (a) show measured values and have no physical meaning

ventional DSC signal was treated as has been done by many authors. The part of the signal at temperatures lower than the starting temperature of increase in the heat flow due to the glass transition was linearly extrapolated to higher temperatures. The extrapolated values can be considered as the heat flow of hypothetical glassy state neglecting the coupling between the local thermal vibration and the degree of freedom of conformational change. Difference between the observed signal and the extrapolated values are considered to be proportional to the heat flow increase accompanying the glass transition. The proportional coefficient depends on temperature. However, the temperature dependence is moderate and the localized change in heat flow due to the glass transition is not affected notably. The linear fitting to the original data from Poly(VB-PSt2530)-570 in Table 1 and the calculated results scaled to the value at 130°C are shown in Figs 2a and b. These two graphs are essentially the same with each other but it is easy to see that Fig. 2b exhibits the characteristic features of the heat flow increase more clearly.

Since only the sample side was modulated in this work the next equation can be used for the cyclic component [16].

$$\frac{1}{T_{\mathrm{cyc}}} = aC - b \tag{1}$$

where T_{cyc}, C, a and b are the complex amplitude of the cyclic component of the measured signal, complex heat capacity of the sample and the complex calibration parameters, respectively. From Eq. (1) we obtain the next equation.

$$\frac{\dfrac{1}{T^{\mathrm{x}}_{\mathrm{cyc}}(T)} - \dfrac{1}{T^{\mathrm{s}}_{\mathrm{cyc}}(T)}}{\dfrac{1}{T^{\mathrm{x}}_{\mathrm{cyc}}(T_0)} - \dfrac{1}{T^{\mathrm{s}}_{\mathrm{cyc}}(T_0)}} = \frac{C_{\mathrm{x}}(T) - C_{\mathrm{s}}(T)}{C_{\mathrm{x}}(T_0) - C_{\mathrm{s}}(T_0)} \tag{2}$$

where x and s designate the unknown sample and the standard material, respectively.

Equation (2) means that one can calculate the difference between the complex heat capacities of the unknown sample and the standard material scaled to the value at the reference temperature T_0 from the results of measurement of the unknown sample and the reference material. In this work T_{cyc} of the glassy state was used as the value of the standard material. Temperature dependence of the real and imaginary parts of $1/T_{\mathrm{cyc}}$ at temperatures lower than the starting temperature of the glass transition was approximately expressed by linear function of the temperature. The values of $1/T_{\mathrm{cyc}}$ at temperatures higher than the starting temperature of the glass transition were calculated from the linear function. Figures 3a and b show the linear fitting to the real and imaginary parts of $1/T_{\mathrm{cyc}}$ measured from Poly(VB-PSt2530)-570. Temperature range in which curvature of the temperature dependence of the real and imaginary parts could be neglected was used for the linear fitting of each sample. In this work the amplitude of the denominator of the left hand side of Eq. (2) was calculated at 130°C. The phase was determined to make calculated values of the left hand side of Eq. (2)

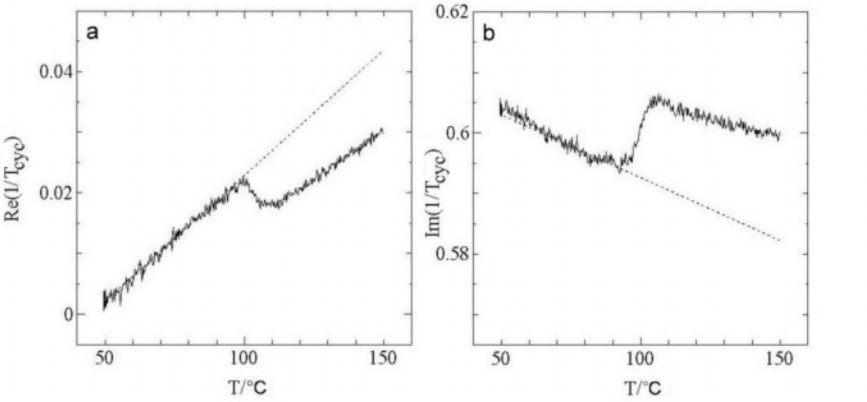

Fig. 3 a – Linear fitting (dotted) to the inverse of the cyclic component, written as T_{cyc}, obtained from the same sample with Fig. 2. a and b – show temperature dependence of the real and imaginary parts, respectively. Numeric values of the vertical axes show measured values and have no physical meaning

be close to real values at temperature higher than ending of the glass transition. Calculated temperature dependence of the difference of the complex heat capacity is shown in Fig. 4, in which δC, $\delta C'$ and $\delta C''$ are defined as $C_x - C_s = \delta C = \delta C' - i\delta C''$. Step increase in $\delta C'$, which is shifted upwards by 0.3 to avoid overlapping, and peak $\delta C''$ can be seen clearly.

The real part of the complex heat capacity times the constant underlying heat flow gives the reversing heat flow as far as the imaginary part can be neglected. Since both the total heat flow shown in Fig. 2b and the complex heat capacity shown in Fig. 4 were scaled to the value at 130°C the real part of the complex heat capacity can

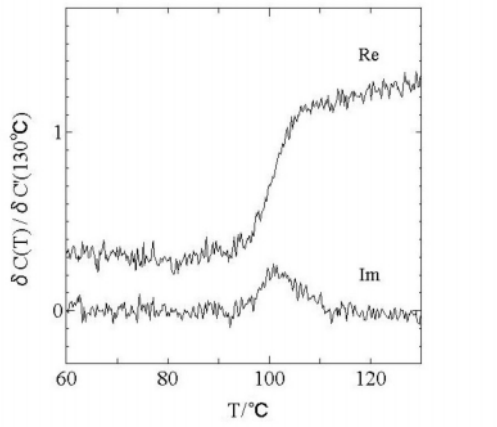

Fig. 4 The complex heat capacity of the blend of LPSt70k and Poly(VB-PSt2530)-570 scaled to the value of the real part at 130°C plotted *vs*. temperature. Re and Im curves are the real and imaginary parts, respectively. The Re curve is shifted upwards by 0.3 to avoid overlapping

be regarded as the reversing heat flow scaled to the value at 130°C. The non-reversing heat flow was calculated by subtracting the reversing heat flow from the total heat flow. The total heat flow, reversing heat flow and the non-reversing heat flow are shown in Fig. 5, in which the total heat flow and the reversing heat flow are shifted upwards by 2 and 1, respectively, to avoid overlapping. The endothermic peak according to the enthalpy relaxation is clearly separated from the step increase of the reversing heat flow. Curves in Fig. 5 are smoother than the curves in Figs 2b and 4. The data of Figs 2b and 4 were averaged over a temperature range of 1 K to obtain the value at every one degree starting 60°C. The data of Figs 2b and 4 were measured independently and the temperature of each data point was not identical to each other. Therefore this procedure was necessary to obtain the non-reversing heat flow.

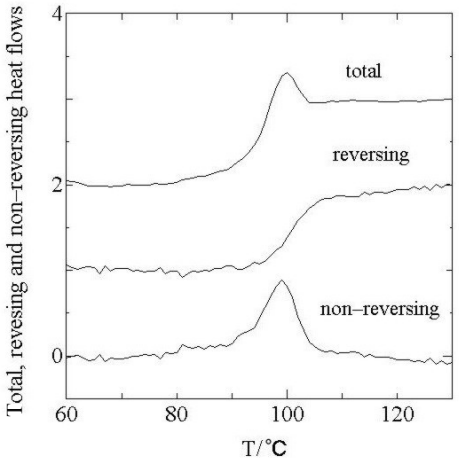

Fig. 5 Temperature dependence of the total heat flow, the reversing heat flow and the non-reversing heat flow of the blend of LPSt70k and Poly(VB-PSt2530)-570. The total heat flow and the reversing heat flow are shifted upwards by 2 and 1, respectively, to avoid overlapping

Figure 6 shows the complex heat capacity, the total heat flow, the reversing heat flow and the non-reversing heat flow measured from other samples in Table 1. The real part of the complex heat capacity, the total heat flow and the reversing heat flow curves are shifted upwards as Figs 4 and 5. In Fig. 7 results from the heating and cooling processes are shown. Frequency dependence is shown in Fig. 8.

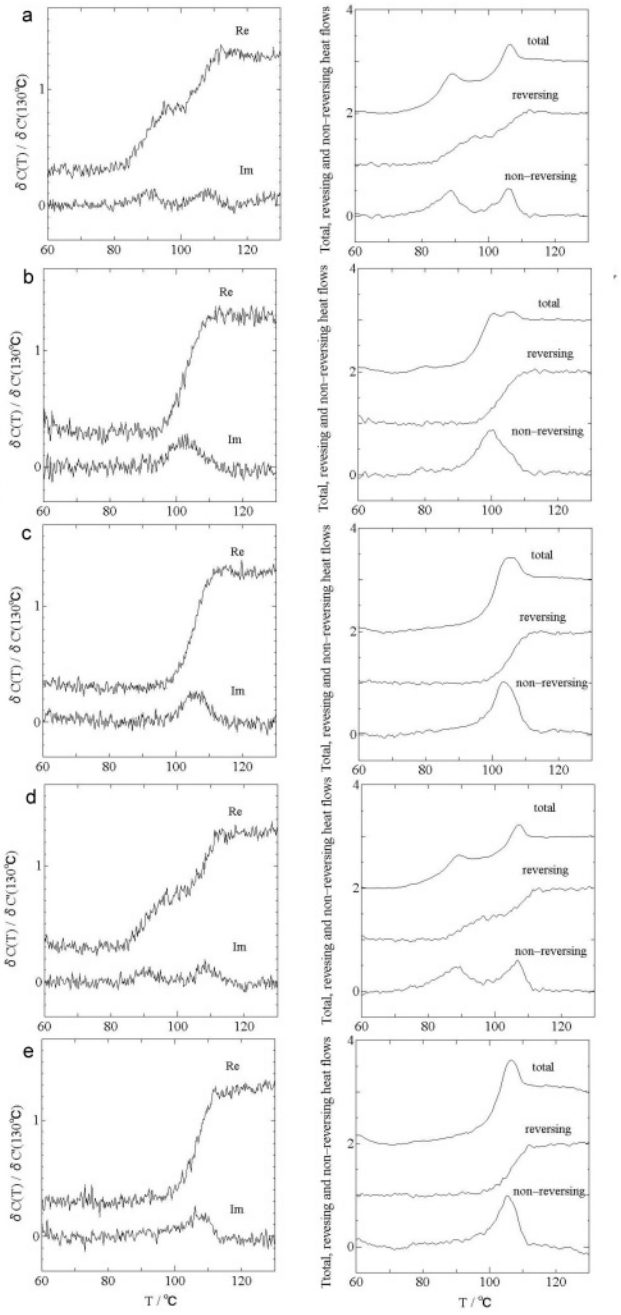

Fig. 6 Similar data to Figs 4 and 5 obtained from the blends of LPSt70k and poly(macromonomer)s listed in Table 1 excepting Poly(VB-PSt2530)-570. a – Poly(MA-PSt1750)-2334; b – Poly(MA-PSt2950)-600; c – Poly(MA-PSt4700)-930; d – Poly(VB-PSt1750)-197 and e – Poly(VB-PSt6200)-739

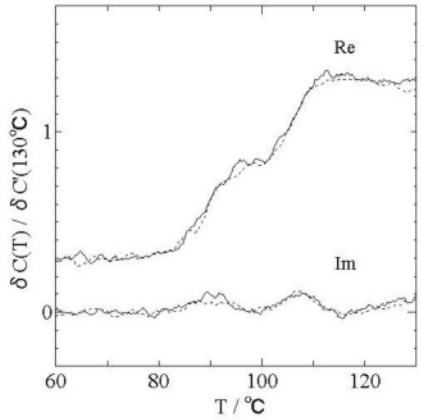

Fig. 7 The complex heat capacity of the blend of LPSt70k and Poly(MA-PSt1750)-2334 measured on the heating (solid) and cooling (dotted) processes. The heating curves are the same with Fig. 6a

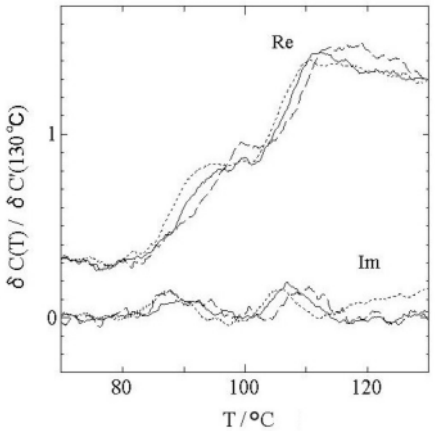

Fig. 8 Frequency dependence of the complex heat capacity of the blend of LPSt70k and Poly(MA-PSt1750)-2334. Modulation period of the dotted, solid and broken curves is 30, 10 and 3 s, respectively. The 10 s curve is the same with Fig. 6a

Discussion

Miscibility of the binary polymer blends can be checked by the number of glass transition. Figures 6a and d clearly show two glass transitions. The real part of the complex heat capacity, which is identical with the reversing heat flow, exhibited two-step increase. The total heat flow, the non-reversing heat flow and the imaginary part of the complex heat capacity had two peaks. All of these results showed that the system was segregated into two phases but this could be known from the conventional DSC measurement as well. Benefits of the LMDSC measurement can be seen in the results of Figs 6b and c. The shape of the endothermic peak due to the enthalpy relaxation

observed in the total heat flow suggested existence of two glass transitions, but relative magnitude of the two endotherms was difficult to be judged from this curve. The non-reversing heat flow elucidated that the lower temperature peak was more notable than the higher one.

Comparison of the relative magnitude of the two glass transitions was rather difficult using the peak of the imaginary part. But this does not mean that separation into the reversing and non-reversing heat flows is always more useful than measurement of the complex heat capacity. It should be stressed that although both the non-reversing heat flow and the imaginary part exhibit a peak (or peaks) at the glass transition temperature the origin of the peak(s) is entirely different from each other. The peak of the non-reversing heat flow is due to the thermodynamically irreversible process from the stabilized glass to the equilibrium liquid. On the other hand the peak of the imaginary part reflects the kinetic properties of the equilibrium state of the sample. Therefore the peak of the imaginary part can be observed in the cooling process as well as the heating process as shown in Fig. 7, in which the solid and dotted curves show the heating and cooling processes of Poly(MA-PSt1750)-2334, respectively. In many cases the equilibrium property is more useful than the irreversible phenomenon to construct a physical model of the system. The complex heat capacity is more useful for that purpose than the reversing and non-reversing heat flows. A typical example of advantage of the complex heat capacity is the frequency dependence [17]. Results at the modulation period of 3, 10 and 30 seconds are shown in Fig. 8. The observed signal was rather noisy for sufficiently quantitative analysis but frequency dependence could be seen apparently.

The shape of the peak of the imaginary part and the non-reversing heat flow seems to give detailed information. The peaks in Figs 4 and 5 are almost symmetric to the peak temperature. On the other hand the peaks in Fig. 6e have a long tail to the lower temperature direction. There is not notable difference between the total heat flow curves in Figs 5 and 6e. Explanation of the long tail is beyond the scope of this paper but characteristic properties of the glass transition of this type of polymer blends might be reflected in the shape of the peaks. Detailed studies about the phase behavior of blends of poly(macromonomer)s and linear polymers will be reported elsewhere.

As described above the simplified method could give useful information about the glass transition of the polymer blends. This simplified method much reduced the measurement and data processing time. Of course there is information which can not be obtained by this method. For example quantitative measurement is necessary to evaluate the rigid amorphous fraction in the crystalline polymers. It is important to be aware of both the possibility and the limitation of this convenient method.

References

1 M. Nishikawa and Y. Saruyama, Thermochim. Acta, 267 (1995) 75.
2 Y. Saruyama, J. Therm. Anal. Cal., 54 (1998) 687.
3 Y. Saruyama, Thermochim. Acta, 330 (1999) 101.
4 Y. Saruyama, J. Therm. Anal. Cal., 59 (2000) 271.

5 Y. Saruyama, Thermochim. Acta (in press).
6 Y. Tsukahara, K. Mizuno, A. Segawa and Y. Yamashita, Macromolecules, 22 (1989) 1546.
7 Y. Tsukahara, K. Tsutsumi, Y. Yamashita and S. Shimada, Macromolecules, 22 (1989) 2869.
8 Y. Tsukahara, K. Tsutsumi, Y. Yamashita and S. Shimada, Macromolecules, 23 (1990) 5201.
9 K. Tsutsumi, Y. Okamoto and Y. Tsukahara, Polymer, 35 (1994) 220.
10 Y. Tsukahara, K. Yai and K. Kaeriyama, Polymer, 40 (1999) 729.
11 Y. Tsukahara, K. Tsutsumi and Y. Okamoto, Macromol. Chem., Rapid Commun., 13 (1992) 409.
12 Y. Tsukahara, S. Namba, J. Iwasa, Y. Nakano, K. Kaeriyama and M. Takahashi, Macromolecules, 34 (2001) 2624.
13 Y. Tsukahara, M. Miyata, K. Senoo, N. Yoshimoto and K. Kaeriyama, Polymers for Advanced Technologies, 11 (2000) 210.
14 Y. Tsukahara, J. Inoue, Y. Ohta and S. Kohjiya, Polymer, 35 (1994) 5785.
15 S. Wakiyama, Thesis for the master degree of Kyoto Institute of Technology (2001) (in Japanese).
16 Y. Saruyama, Thermochim. Acta, 282/283 (1996) 157.
17 N. O. Birge, Phys. Rev., B34 (1986) 1631.